Available online at www.sciencedirect.com

ScienceDirect

Procedia Earth and Planetary Science 17 (2017) 484 – 487

Procedia Earth and Planetary Science

15th Water-Rock Interaction International Symposium, WRI-15

Tracing U mobility in deep groundwater using Ra isotopes

L. Krall[a,1], L. Auqué[b], E.L. Tullborg[c], J. Suksi[c], G. Trezzi[d], J. Garcia-Orellana[d], P. Andersson[e], D. Porcelli[f]

[a]*SKB, Box 250, 10124 Stockholm, Sweden*
[b]*Department of Earth Sciences, University of Zaragoza C/Pedro Cerbuna 12, 50009 Zaragoza, Spain*
[c]*Sweden Terralogica, AB, Östra Annekärrsvägen 17, SE-443 72 Gråbo, Sweden*
[d]*Institut de Ciència i Tecnologia Ambientals, Universitat Autònoma de Barcelona, 08193 Cerdanyola del Vallès, Barcelona, Spain*
[e]*Naturhistoriska Riksmuseet, Box 50007 10405 Stockhoom, Sweden*
[f]*Department of Earth Sciences, University of Oxford, South Parks Road OX1 3AN, United Kingdom*

Abstract

The mobility of natural U is compared among four boreholes in a fractured granite using Ra isotopes and geochemical modelling. $^{222}Rn/^{226}Ra$ activity ratios (ARs) spanning an order of magnitude underline differences in reactive surface area. $(^{224}Ra/^{228}Ra)_{ARs}$ up to 9 indicate recent changes in hydrogeochemistry, and $(^{226}Ra/^{228}Ra)_{ARs}$ 0.6-30 indicate variable deposition of U. Dissolved U is related to dissolution of a solid U(VI) phase by groundwater with HCO_3^- >20 mg·L^{-1}. U reduction is hindered by $Ca_2UO_2(CO_3)_3^0$.

Peer-review under responsibility of the organizing committee of WRI-15

Keywords: Uranium, $Ca_2UO_2(CO_3)_3^0$, crystalline bedrock, Ra isotopes, spent nuclear fuel

1. Introduction

The Swedish Nuclear Fuel and Waste Management Co. (SKB) has applied to construct a spent nuclear fuel repository ~500 meters below sea level (m.b.s.l.) in Forsmark, Sweden[1]. The mobility of natural U at the site must be understood to assess the performance of a repository. Elevated (>10 µg/L) dissolved natural U in Fe(II) containing Forsmark groundwaters (~500 m.b.s.l.) with >20 mg/l HCO_3^- has prompted an investigation of U and its nuclides[2].

Forsmark is dominated by fractured calc-alkaline crystalline bedrock (~1.85 Ga). Groundwaters evolved from five endmembers: current meteoric and minor present Baltic Sea (20-200 m.b.s.l.), post-glacial Littorina Sea (9000-

* Corresponding author. Tel.: +46-7-0254-0560.
E-mail address: Lindsay.Krall@skb.se

Peer-review under responsibility of the organizing committee of WRI-15
doi:10.1016/j.proeps.2016.12.122

5000 B.P.) mixed with glacial meltwater (200-700 m.b.s.l.), and deep saline water (>700 m.b.s.l.)[3]. Dissolved U originates from a solid U-phase in the fracture network. U(IV), initially deposited in local pegmatites, was oxidized by hydrothermal fluids (>1Ga). The U(VI) precipitated in haiweeite and uranophane, which were altered by carbonate-rich fluids[4].

Ra isotopes, produced by U and Th progenitors in the aquifer, have identical chemical properties and physical relationships which can be exploited to study aquifer properties and processes on timescales similar to the half-lives of the applied radionuclides (~4d to 1.6ky; Fig. 1)[5]. Here, speciation-solubility calculations are complemented by Ra isotope systematics to study water-rock interaction on timescales ranging from the intrusion of HCO_3^--rich Littorina seawater (5-6 ka) to the present day to understand the processes and timescales of U mobility at Forsmark.

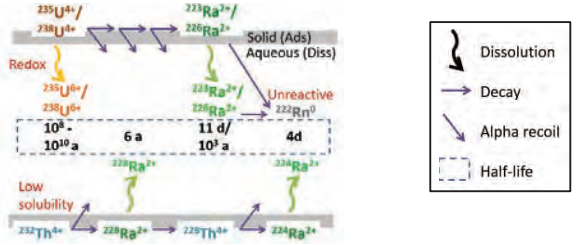

Fig. 1. U/Th decay series schematic showing relations between Ra isotopes in solid and aqueous phase.

2. Methods

Groundwaters were collected from boreholes (~500 m.b.s.l.) drilled during the Forsmark site investigation (2002-2008). Elemental, ^{226}Ra, and ^{222}Rn data were available through the SKB database Sicada. Speciation-solubility calculations were performed in Phreeqc[6] using the Thermochimie thermodynamic database[7]. This database contains stability constants for $CaUO_2(CO_3)_3^{-2}$ and $Ca_2UO_2(CO_3)_3^0$, the latter of which have now been identified in Forsmark groundwater[8]. In 2015, ^{223}Ra, ^{224}Ra, ^{226}Ra, and ^{228}Ra were sampled and measured at the Universitat Autònoma de Barcelona (UAB) using Radium Delayed Coincidence Counting (^{223}Ra, ^{224}Ra) and gamma spectroscopy (^{226}Ra, ^{228}Ra).

3. Results and discussion

Four deep borehole sections were examined: 1) KFM02A (high HCO_3^-+U), 2) KFM03A (medium HCO_3^-+U), 3) KFM08A (low HCO_3^-+U), 4) KFM01D (medium HCO_3^-+low U). Only Sicada datasets reporting ^{226}Ra and ^{222}Rn were considered. Table 1 shows average HCO_3^-, U, and additional modelling parameters and results, as well as Ra and Rn activities. Sicada data are averaged over *n*, while UAB Ra data represent single samples. Solid-phase Ra was not measured, but dissolved Ra and Rn activities are used in activity ratios (ARs) together with geochemistry to understand the solid phases in the fracture network and water-rock interaction. Subscripts "Diss" and "Ads" refer to a dissolved or solid phase activity, respectively, and "Tot" to the total activity of a nuclide the borehole section ("Diss" + "Ads").

Table 1: Mean (μ) and standard deviations (σ) of selected groundwater data (sample size *n*), including ^{226}Ra and ^{222}Rn activities and Phreeqc results. Analytical uncertainties given for UAB data (σ). TDS = total dissolved solids, Brt = barite, Cc = calcite. $pE_{calc.}$, Fe and S, see text.

		g·L^{-1}	mg·L^{-1}			μg·L^{-1}		Saturation index		Eh (mV)		Sicada		UAB	(dpm·100L^{-1})		
	pH	TDS	Ca	HCO_3^-	Fe	Ba	U	Brt	Cc	Fe	S	^{226}Ra	^{222}Rn	^{226}Ra	^{223}Ra	^{228}Ra	^{224}Ra
			·10^3									·10^4	·10^6	·10^4	·10^2	·10^3	·10^3
KFM02A, n = 5																	
μ	7.2	9.7	1.0	130	2.0	89	157	0.4	0.09	-216	-191	2.1	14	1.3	7.7	5.7	5.1
σ	0.1	0.1	0.0	2.3	0.3	6.4	13	0.02	0.2	37	14	0.5	2.7	0.1	0.5	0.4	0.5
KFM03A, n = 5																	
μ	7.5	9.5	1.5	26	0.8	160	43	0.3	-0.04	-265	-224	11	44	9.5	91	3.2	30
σ	0.0	0.1	0.0	5.6	0.1	9.4	7.1	0.05	0.2	20	8.3	2	17	0.7	8	0.3	3
KFM08A, n = 4																	

μ	8.2	10	2.0	13	0.4	360	5.0	0.3	0.07	-308	-256	3.1	2.7	2.6	19	9.1	12
σ	0.3	0.0	0.0	2.3	0.2	1.8	3.3	0.05	0.6	97	31	1	0.1	1.0	2	0.5	1
KMF01D, n = 2																	
μ	7.6	7.5	1.3	44	0.7	680	1.4	0.7	-0.1	-206	-218	2.5	4.2	8.8	37	140	72
σ	0.2	0.7	0.1	11	1.0	110	0.7	0.1	0.2	53	20	0.1	2.2	0.5	4	8	8

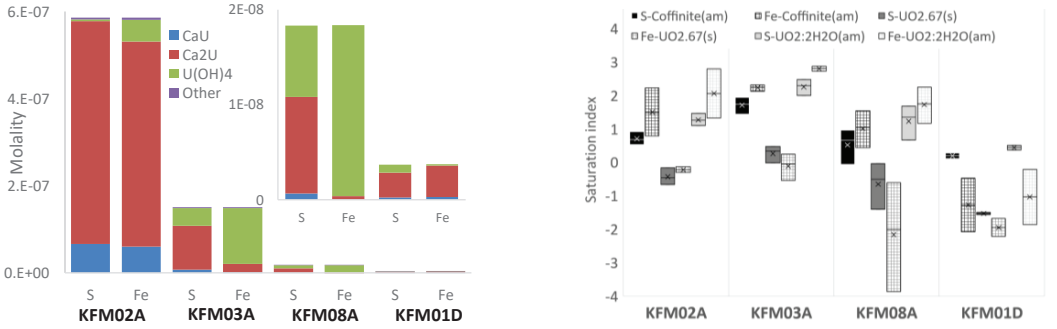

Fig. 2. Calculated (a) aqueous speciation and (b) saturation indexes of U solid phases using Fe and S redox couples.

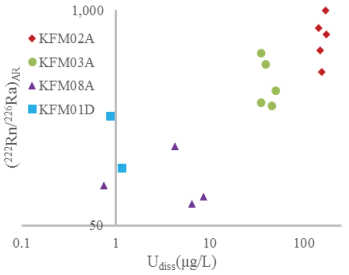

Fig. 3. $(^{222}Rn/^{226}Ra)_{AR}$ versus total dissolved U (Sicada)

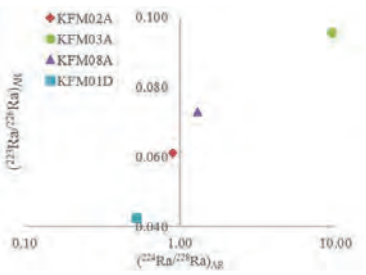

Fig. 4. $(^{223}Ra/^{226}Ra)_{AR}$ versus $(^{224}Ra/^{228}Ra)_{AR}$

3.1. Speciation-solubility calculations

In each section, barite was slightly over-saturated and calcite was in equilibrium. Total dissolved solids were ~10 $g{\cdot}L^{-1}$. Redox potentials (Eh) were calculated from the $Fe(OH)_{3(s)}/Fe^{+2}$ (Fe)[8] and the $S(-2)/SO_4^{2-}$ (S) redox couples. Resulting potentials agreed well with the in-situ Eh measurements[9]. Redox potentials are more negative and also more sensitive to the selected couple in KFM03A and KFM08A than in KFM02A and KFM01D.

The speciation of U, particularly between $Ca_2UO_2(CO_3)_3^0$ and $U(OH)_4$, was sensitive to the redox selection (Fig. 2a). Irrespective of the selected couple, $Ca_2UO_2(CO_3)_3^0$ predominated in KFM02A. In KFM03A, the speciation was more complex, resulting in ~25% and 90% $U(OH)_4$ for the S and Fe couples, respectively. It appears unlikely that so high a proportion U(IV) is present in a solution with such high dissolved U.

Saturation indices (SI) of the U-bearing solid phases were less sensitive to the redox selection (Figure 2b). An amorphous UO_{2+x} was in equilibrium in KFM02A and KFM03A. Amorphous coffinite and an amorhpous hydrous U(IV) ($UO_2{:}2H_2O_{(am)}$) phase are oversaturated in all except KFM01D. All samples were under-saturated with respect to uranophane (-6 <SI< -3), whose SI was more dependent on alkalinity than on redox.

3.2. Ra and Rn ARs

$^{222}Rn/^{226}Ra$ ARs can be used to attribute elevated U_{Diss} to a low adsorption potential (i.e. reactive surface area) of the local aquifer solids or to the aqueous speciation of U, i.e. the presence of low-sorbing $Ca_2UO_2(CO_3)_3^0$. $^{226}Ra_{Diss}$ alone does not indicate a reactive surface area because the $^{226}R_{tot}$, which depends on $^{226}Ra_{Ads}$, is unknown. However, ^{222}Rn, sourced by $^{226}Ra_{Diss}$ and $^{226}Ra_{Ads}$, is unreactive so principally available as $^{222}Rn_{Diss}$ (Fig. 1). Linking $^{222}Rn_{diss}$ to $^{226}Ra_{tot}$, $^{226}Ra_{Ads}$ can be inferred from the $(^{222}Rn/^{226}Ra)_{AR}$, which is proportional to the reactive surface area[5].

A relationship is observed between $(^{222}Rn/^{226}Ra)_{AR}$ and U_{Diss} (Fig. 3). This suggests that the reactive surface area is actually greater where U_{Diss} is elevated than where U_{Diss} is low, which is likely a result of the high fracture frequency around the KFM02A and KFM03A zones relative to the KMF08A and KFM01D zones. It appears that, particularly in KFM02A, U adsorption is hindered by aqueous speciation rather than by a low reactive surface area.

$^{224}Ra/^{228}Ra$ ARs and $^{223}Ra/^{226}Ra$ ARs indicate whether the system has returned to steady state after a change in the hydrologic regime. ^{224}Ra and ^{223}Ra are produced and recoiled into solution, and arrive at a constant groundwater activity more rapidly than ^{228}Ra and ^{226}Ra. Similarities between ^{223}Ra and ^{226}Ra production through their respective decay chains should result in a steady state $^{223}Ra/^{228}Ra$ AR of .046 after ~8000 y. Similarly, ^{224}Ra is replenished by local ^{228}Th more rapidly than ^{228}Ra by ^{232}Th, so $(^{224}Ra/^{228}Ra)_{ARs}$ >~1-2 indicate recent disruption in groundwater flow[5].

The positive relationship between $(^{223}Ra/^{226}Ra)_{AR}$ and $(^{224}Ra/^{228}Ra)_{AR}$ (Fig. 4) demonstrates that these ARs are driven by the state of the Ra systems, rather than by e.g. sorption kinetics. No relationship between AR and alkalinity or dissolved U has been observed (Table 1). KFM01D is in steady state with respect to both $^{226}Ra_{diss}$ and $^{228}Ra_{diss}$. $^{226}Ra_{diss}$ is not in steady state in KFM02A and KFM08A. Therefore, these groundwaters were replenished within the past 8000 y. KFM03A has not reached steady state with respect to $^{228}Ra_{diss}$, so this groundwater in this borehole section was replenished < 10 years ago.

$^{226}Ra/^{228}Ra$ ARs can be used to determine the U/Th ratio of the local fracture surfaces because ^{226}Ra and ^{228}Ra are progeny of ^{238}U and ^{232}Th, respectively. The average $(^{238}U/^{232}Th)_{AR}$ of the upper crust is ~0.8. $(^{226}Ra/^{228}Ra)_{ARs}$ in groundwater should be similar but may increase where U has been mobilized[5]. The maximum $(^{226}Ra/^{228}Ra)_{AR}$ was observed in KFM03A (~30). Although KFM02A had the highest HCO_3^- and dissolved U contents, the $(^{226}Ra/^{228}Ra)_{AR}$ was only ~2, which suggests that the extent of secondary U deposition on the fracture surface near KFM02A is low relative to KFM03A. In KFM01D, an AR ~0.6 is similar to the average crust and thus indicative of low U mobility.

4. Conclusions

Integrated speciation-solubility calculations and Ra-Rn systematics support the following working hypotheses:

- In borehole section KFM02A, U_{Diss} is driven by HCO_3^--rich Littorina groundwaters. ARs were disrupted around the time of seawater intrusion. Uranophane is under-saturated, and elevated U_{Diss} is maintained by $Ca_2UO_2(CO_3)_3^0$ complexation.
- Borehole section KFM03A, with lower HCO_3^- and lower redox potential alongside $(^{226}Ra/^{228}Ra)_{ARs}$ ~30, is a zone of U deposition. Destabilization of $Ca_2UO_2(CO_3)_3^0$, elevated UOH_4, and disruption of ^{228}Ra <10a suggests geochemical disequilibrium.
- Major U oxidation by hydrothermal fluids did not occur in the zone around borehole section KFM01D, given the $(^{226}Ra/^{228}Ra)_{AR}$ of ~0.6. Thus, a $U(VI)_{solid}$ phase is not available for dissolution by the HCO_3^- -containing groundwater.

Acknowledgments

This study was funded by SKB and the EU FP7 Marie Curie Network, MetTrans.

References

1. SKB, 2008. *Report SKB TR-08-05*, Swedish Nuclear Fuel and Waste Management Co., Stockholm
2. Sandström, B., Tullborg, E.-L., Smellie, J. 2008. *Report SKB R-08-102*, Swedish Nuclear Fuel and Waste M Management Co, Stockholm.
3. Laaksoharju, M., Smellie, J., MacKenzie, A.B., Suksi, J., Tullborg, E.-L., Gimeno, M., Hallbeck, L., Molinero, J., Waber, N., 2008: *Report SKB R-08-47.* Swedish Nuclear Fuel and Waste Management Co, Stockholm.
4. Krall L., Sandström B., Tullborg E-L, Zetterström-Evins L. 2015. *Applied Geochemistry*, 59, 178-188.
5. Porcelli D., 2008. *Radioactivity in the Evironment*, 13, 105-153.
6. Parkurst, D.L. and Appelo, C.A.J. (2013). Description of input and examples for PHREEQC, Version 3. Chapter 43 of Section A, Groundwater Book 6, Modeling Techniques. Techniques and Methods 6–A43. U.S. Geological Survey.
7. Giffaut, E., Grive, M., Blanc, Ph., Vieillard, Ph., Colas, E., Gailhanou, H., Gaboreau, S., Marty, M., Made, B., and Duro, L. 2014. *Applied Geochemistry*, 49, 225-236.
8. Tullborg, E-L., Suksi, J., Geipel, G., Krall, L., Auqué, L., Gimeno, M., Puigdomenech, I. The occurrences of $Ca_2UO_2(CO_3)_3$ complex in Fe(II) containing deep groundwater at Forsmark, eastern Sweden, submitted to WRI-15. 2016.
9. Gimeno, M.J., Auqué, L.F., Gómez, J., Acero, P. 2008. *Report SKB R-08-86*, Swedish Nuclear Fuel and Waste Management Co, Stockholm.